In-vivo Comparison of B1 Shimming and Spatially Tailored Parallel Excitation at 7T.

V. Alagappan[1,2], K. Setsompop[3], A. Potthast[4], U. J. Fontius[5], F. Schmitt[5], E. Adalsteinsson[3], and L. L. Wald[1]

[1]Athinoula A. Martinos Center for Biomedical Imaging, Charlestown, MA, United States, [2]Biomedical Engg, Tufts University, Medford, MA, United States, [3]EECS, MIT, Cambridge, MA, United States, [4]Siemens Medical Solutions, Charlestown, United States, [5]Siemens Medical Solutions, Erlangen, Germany

Introduction: The inhomogeneous transmit (B_1^+) pattern in conventional volume coils at higher field strengths has motivated the development of RF excitation strategies employing multiple transmit channels. The array approach allows mitigation of the B_1^+ field inhomogeneity either directly by B1 shimming (1), or by using accelerated spatially tailored 2D or 3D RF pulses to control the excitation profile(2,3,4). A 3D echovolumar trajectory provides slice-selective excitation in z and modulation of the excited magnetization in the (x,y) plane depending on the B_1^+profiles and the amplitude and phases of the sinc-like pulses played out on each of the k_z "spokes"(5). This trajectory allows simple comparison to RF shimming since the shimming can be cast as a single-spoke excitation at $(k_x,k_y) = (0,0)$. In both cases, the phases and amplitudes of the pulses on each spoke trajectory are optimized in a magnitude least-square sense with respect to a uniform target profile (6). In this work we compare the ability of the two methods to achieve uniform slice-selective excitations in water phantoms (sphere and head-shaped) as well as in the human head using 8 transmit channels and a stripline TX head array.

Methods: The experiments were performed on a Siemens 7T system equipped with 8 transmit channels. A 16 channel stripline array coil (length 15cm, dia. 28cm) was constructed with a strip width of 2.54cm, shield width 5cm, and 1.3cm of Teflon spacing. Adjacent elements were capacitively decoupled. Only every other element was used in this study, with the TX ports of the remaining elements terminated. The comparison where performed on a spherical saline phantom (1.25g/l of $NiSO4.6H_2O$ and 5g/l of NaCl) a head shaped saline phantom (1.25g/l of $NiSO4.6H_2O$ and 2.6g/l of NaCl) and *in-vivo* in human subject with IRB approval, informed consent and a very conservative ("worst case") SAR monitoring system.

Quantitative B_1^+ mapping was performed by first measuring the proton-density weighted receive profile (B_1^-) of the birdcage-like reception mode of the array as well as the B_1^+ transmit profile when the excitation is phased in a birdcage (uniform mode) relationship. The uniform birdcage transmit mode is formed by setting the phase-shifts of the transmit channels in 45 degree increments and uniform amplitude. The uniform birdcage receive mode was formed by appropriately phasing and combining the fully relaxed (TR=10s) complex image data. Quantitative information about the B_1^+ and B_1^- maps of this uniform BC mode was derived from images acquired with 4 different TX voltage levels (20V, 40V, 60V and 80V). The image intensities were fitted to the expected $\sin(\alpha)$ dependence on flip angle for fully relaxed images. The map formed from the proportionality constant in this fit represents a combination of M_0 and the B_1^- profile. Thus the map of $|B_1^-|$ is found. The complex B_1^+ maps for each channel were then found by obtaining a low flip-angle, fully relaxed image with single channel excitation and dividing this image by the $M_o|B_1^-|$ map. The B_1^+ maps formed in this way all contain the additional phase roll imposed by the uniform BC mode reception (only the magnitude of B_1^- is divided out). This phase roll is unimportant since it is identical on all channels and the final images will be analyzed for magnitude B_1^+ homogeneity only. Although complicated, this B_1^+ mapping method is advantageous since the time-consuming acquisition of images at multiple excitation voltages is only performed one time (rather than for each channel). The excitation maps (TX_{map}) created by the B_1^+ mitigation strategies were obtained by acquiring a low-flip angle gradient echo fully relaxed magnitude images using the uniform BC reception arrangement and dividing by the measured $|B_1^-|$ map.

The excitation trajectory consisted of a 3D k-space excitation using a either 2 or 3 line segments or "spokes" in k_z, placed symmetrically in the (k_x,k_y) plane (Fig.1). The RF pulse duration for 1-spoke, 2-spoke and 3-spoke trajectories where 1ms, 1.7ms and 2.4 ms respectively. Use of a sinc-like RF waveform during the transversal of each spoke achieves a sharp slice-selection in z. When only a single spoke is used at $k_x,k_y = 0$ this trajectory is a simple slice selective excitation and optimization of the phase and amplitude of each TX channel by the algorithm achieves B_1 shimming. The optimization of the multi-channel pulses with respect to the uniform target excitation profile given the B_1^+ maps was performed using the spatial domain formalism of Grissom et al (7).

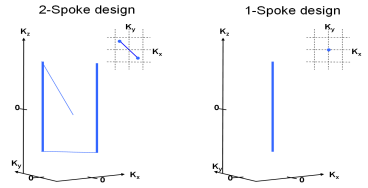

Fig 1 : The 2-spoke and 1-spoke gradient trajectories.

Results & Conclusion: Fig. 2 shows the B_1^+ magnitude and phase maps of the 8 elements used for excitation. The S_{12} decoupling between the adjacent elements was -18dB and that for the next nearest neighbors was -12 dB; similar to that of a gapped 8 channel stripline array coil. Fig. 3 shows the flip-angle homogeneity achieved on the two phantoms and human head. The first column is the $|TX_{map}|$ maps from standard slice-select excitation using the appropriate birdcage mode for both TX and RX ($BC_{TX/RX}$). The second column shows $|TX_{map}|$ maps for the same slice-select excitation with birdcage reception, but B_1^+ mitigation with RF shimming. The third column shows $|TX_{map}|$ maps for the spatially tailored pulses (2 spokes in the sphere and human and 3 spokes in the head-shaped phantom). Standard deviation (as % of mean) of the $|TX_{map}|$ were 28.3% ($BC_{TX/RX}$), 14.2% (RF shimming) and to 4.6% (spatially tailored excitation) in the spherical phantom. For the head-shaped phantom, the results were 41.7%, 26.6% and 4.7%. For the human head, the results were 20.6%, 14.1% and 9.7%.

It should be noted that some anatomy remains in the human $|TX_{map}|$, likely from the very long T_1 of CSF at 7T. This exaggerates the standard deviations results for all of the methods *in-vivo*. In all three cases, the spatially tailored pulses give a more uniform flip-angle excitation compared to B_1 shimming at the expense of a slight increase in RF pulse duration.

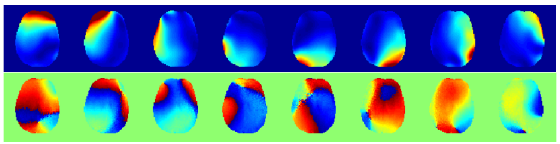

Fig. 2 : The B_1^+ mag and phase profiles

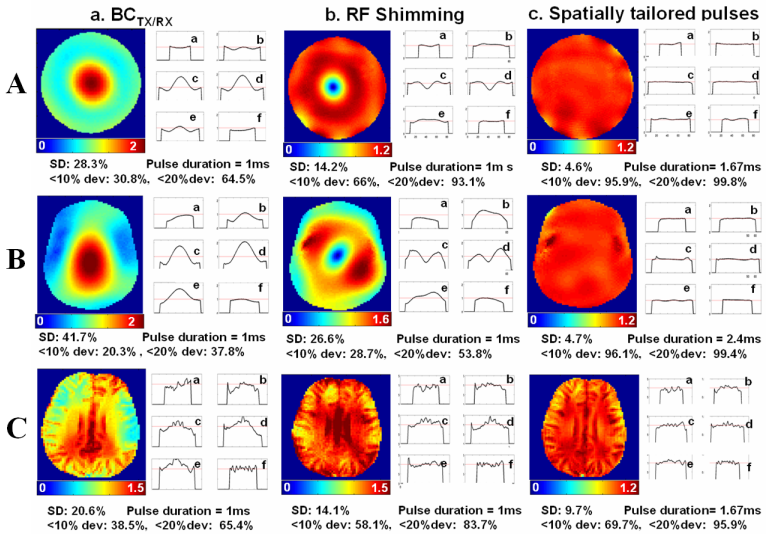

Fig. 3 : B1+ maps on water sphere (A), head shaped water phantom (B) and the human head (C) with Birdcage Tx/Rx, B1 Shimming and spatially tailore excitation. The degree of inhomogeneity represented as a percentage standard deviation over the mean.

References: 1) Adriany et al MRM 53(2) P 434, 2) Pauly et al JMR 1989 81 p43, 3)Katcher et al, MRM 2003 49(1) p 144, 4) Zhu et al MRM 2004 51(4) p775 5) Saekho et al,MRM 2005 53(2) p474 6) Setsompop et al MRM 2006 56(5) P 1163 7) Grissom et al MRM 2006 56(3) P 620